TOA and TDOA-Based Passive Localization Using AIS Signals for Maritime Surveillance

Massimo Marrazzo
University of Naples "Federico II"
Italian Coast Guard Headquarters
Rome, Italy
massimo.marrazzo@unina.it

Vincenzo Carotenuto, Antonio De Maio
Dept. of Electr. Eng. and Inf. Technology (DIETI)
University of Naples "Federico II"
Napoli, Italy
{vincenzo.carotenuto, ademaio}@unina.it

Luca Pallotta
Department of Engineering (DiING)
University of Basilicata
Potenza, Italy
luca.pallotta@unibas.it

***Abstract*—This paper investigates passive localization techniques that utilize physical-layer measurements, specifically Time of Arrival (TOA) and Time Difference of Arrival (TDOA), extracted from Automatic Identification System (AIS) signals intercepted by the Italian AIS Base Station network. The study evaluates three localization algorithms, viz. two classical Least Squares (LS) estimation methods based on TOA and TDOA measurements, and a Constrained Least Squares (CLS) algorithm employing TDOA measurements that integrates bespoke constraints to improve estimation accuracy. Experimental validation using measured AIS data demonstrates that the CLS-TDOA algorithm outperforms the classical LS approaches, providing enhanced positioning accuracy and robustness.**

***Index Terms*—Automatic Identification System (AIS), Least Squares (LS), Constrained Least Squares (CLS), Time Difference of Arrival (TDOA), Time of Arrival (TOA)**

I. Introduction

Maritime localization systems traditionally rely on cooperative techniques, where vessels actively transmit their positional information through the Automatic Identification System (AIS) signals. This cooperation enables accurate tracking and navigation by leveraging the data broadcast by the ships and collected by shore-based/satellite AIS receivers, and AIS Base Stations (BSs). However, a major challenge is that vessels can intentionally transmit false positional information through AIS signals to avoid accurate localization. This kind of deception undermines the reliability of traditional AIS-based localization systems.

To overcome these limitations, passive localization techniques can be used instead of relying on AIS message content. These methods enable the estimation of vessel positions using physical-layer measurements, such as Time of Arrival (TOA) and Time Difference of Arrival (TDOA) [1]–[9], extracted from AIS signals collected at multiple receiving nodes.

In the context of maritime situational awareness, some passive localization algorithms have been adapted and evaluated using AIS signals intercepted by the BSs [10]–[13]. Notably, [10] laid the groundwork by demonstrating the feasibility of AIS signal localization using Extended Kalman Filters (EKF), offering improvements over traditional TDOA-based multilateration methods. Building on this, [11] developed a vessel positioning algorithm that combines TDOA and Frequency Difference of Arrival (FDOA) techniques with an Interactive Multiple Model (IMM) framework to better capture vessel dynamics in satellite-based AIS systems. Additionally, [12] addressed real-world constraints by proposing an asynchronous TDOA algorithm designed for networks of unsynchronized receivers, improving system flexibility in practical maritime environments. Finally, [13] introduced a robust two-step TDOA localization method that mitigates timing attacks and synchronization errors, enhancing both security and reliability. These techniques might improve passive localization using AIS signals and also help to verify reported positions and to detect unusual behavior, such as spoofing, faulty transmitters, or vessels hiding their true identity.

Building on the framework proposed in [10], this paper evaluates and compares the effectiveness of three passive localization algorithms fed with real TOA measurements provided by the Italian AIS network. Specifically, two techniques rely on the classical Least Squares (LS) estimation technique using TOA and TDOA measurements. The third is the Constrained Least Squares (CLS) TDOA algorithm originally proposed in [4], which introduces two constraints into the estimation problem to improve localization accuracy. The performance of these algorithms is experimentally assessed in terms of positioning accuracy using measured data. The results highlight that the CLS-TDOA outperforms the classical LS-based approaches in terms of positioning accuracy, demonstrating improved robustness and precision under real-world conditions. Finally, the impact of the sensor arrangement on localization performance has also been investigated, showing that sensor geometry not only governs the theoretical estimation accuracy but also plays a crucial role in determining the robustness of practical estimators.

The remainder of the paper is organized as follows. Section II formulates the problem and presents the LS and CLS localization algorithms. Section III describes the TOA measurements provided by the Italian AIS network. Section IV discusses the results of experimental analyses, comparing the performance of the considered algorithms. Finally, Section V concludes the paper and outlines directions for future

The work of V. Carotenuto and A. De Maio was supported by European Union under the Italian National Recovery and Resilience Plan (NRRP) of NextGenerationEU, partnership on "Telecommunications of the Future" (PE00000001-Program "RESTART").

© 2025 IEEE. Personal use is permitted, but republication/redistribution requires IEEE permission.
See https://www.ieee.org/publications/rights/index.html for more information

researches.

II. Problem Formulation and System Model

Let us consider a passive vessel localization system consisting of N receiving sensors, each capable of measuring the TOA of AIS signals. Denoting:

- $\boldsymbol{s}_i = [x_i, y_i]^T$, $i = 1, \ldots, N$: the locations of the sensors (assumed to be perfectly known);
- τ_i, $i = 1, \ldots, N$: the measured TOAs;
- $\boldsymbol{u} = [x_u, y_u]^T$: the unknown position of the vessel to be localized;

the following subsections present the observation models for TOA and TDOA localization, along with the considered solution techniques.

TOA measurements form the foundation of many passive localization techniques, as they enable the estimation of the distance between a signal source and a receiver by leveraging the time delay between transmission and reception. However, to be applicable, TOA-based localization techniques require precise knowledge of both the actual TOAs at multiple sensors (τ_i, $i = 1, \ldots, N$) and the time instant at which the transmission from the sources to be localized occurs (referred hereafter as τ_0). Although many algorithms are available to accurately estimate the TOAs, in real-world applications the information about τ_0 is often challenging. This limitation is a key reason why TDOA-based methods are more commonly used, as they rely solely on the relative arrival times of signals at different receivers, thus eliminating the need for knowledge of the absolute transmission time.

Before proceeding further, let us observe that, to be effective, both TOA and TDOA localization methods require precise time synchronization among the N nodes of the passive localization system. In other words, all receiving nodes must share a common clock or be synchronized to a common time reference, ensuring that the measured TOAs are directly comparable across sensors. This assumption is retained throughout the system model formulation for both TOA and TDOA presented in the following subsections.

A. TOA-Based Localization and LS Estimation

Assuming that τ_0 is known, the Euclidean distance r_i between the emitter being localized and the ith receiving sensor (hereafter referred to as range) is related to the TOA measurement via

$$r_i = c(\tau_i - \tau_0) = \|\boldsymbol{s}_i - \boldsymbol{u}\|, \quad i = 1, \ldots, N, \tag{1}$$

where c is the speed of light, and $\|\cdot\|$ denotes the Euclidean vector norm. By squaring both sides of (1), applying standard algebraic manipulations, and defining the unknown parameter vector as

$$\boldsymbol{\theta}_{\text{TOA}} = \begin{bmatrix} \boldsymbol{u} \\ \|\boldsymbol{u}\|^2 \end{bmatrix}, \tag{2}$$

the TOA system model can be approximated in the linear form as

$$\boldsymbol{H}_{\text{TOA}}\boldsymbol{\theta}_{\text{TOA}} = \boldsymbol{a}_{\text{TOA}} \tag{3}$$

where

$$\boldsymbol{H}_{\text{TOA}} = \begin{bmatrix} -2\boldsymbol{s}_1^T & 1 \\ -2\boldsymbol{s}_2^T & 1 \\ \vdots & \vdots \\ -2\boldsymbol{s}_N^T & 1 \end{bmatrix}, \quad \boldsymbol{a}_{\text{TOA}} = \begin{bmatrix} r_1^2 - \|\boldsymbol{s}_1\|^2 \\ r_2^2 - \|\boldsymbol{s}_2\|^2 \\ \vdots \\ r_N^2 - \|\boldsymbol{s}_N\|^2 \end{bmatrix}.$$

Provided that $\boldsymbol{H}_{\text{TOA}}$ is of full column rank, the LS estimator of $\boldsymbol{\theta}_{\text{TOA}}$ is given by

$$\hat{\boldsymbol{\theta}}_{\text{TOA}}^{\text{LS}} = \left(\boldsymbol{H}_{\text{TOA}}^T\boldsymbol{H}_{\text{TOA}}\right)^{-1}\boldsymbol{H}_{\text{TOA}}^T\boldsymbol{a}_{\text{TOA}}. \tag{4}$$

B. TDOA-Based Localization and LS Estimation

To overcome the limitation arising from the possible unavailability of the transmission time τ_0, it is possible to consider the differences between TOA measurements rather than the absolute TOAs themselves. This leads to the TDOA-based localization approach, which relies solely on the relative arrival times of the signal at the different sensors. By eliminating the dependence on the unknown τ_0, TDOA offers a practical alternative in scenarios where the transmission time cannot be directly measured or estimated with sufficient accuracy.

To establish the TDOA-based localization system model, without loss of generality, let us consider the sensor $\boldsymbol{s}_1$ as the reference for the TDOA measurements. By doing so, the available observations are given by

$$\tau_{i1} = (\tau_i - \tau_0) - (\tau_1 - \tau_0), \quad i = 2, \ldots, N, \tag{5}$$

which can be expressed in terms of range-difference measurements as

$$r_{i1} = c\tau_{i1} = r_i - r_1 = \|\boldsymbol{s}_i - \boldsymbol{u}\| - \|\boldsymbol{s}_1 - \boldsymbol{u}\|, \; i = 2, \ldots, N. \tag{6}$$

By squaring the left- and right-hand sides of (6), applying standard algebraic manipulations and considering

$$\boldsymbol{\theta}_{\text{TDOA}} = \begin{bmatrix} \boldsymbol{u} \\ r_1 \end{bmatrix} \tag{7}$$

as the unknown parameter vector, the TDOA system model can be approximated as

$$\boldsymbol{H}_{\text{TDOA}}\boldsymbol{\theta}_{\text{TDOA}} = \boldsymbol{a}_{\text{TDOA}} \tag{8}$$

where

$$\boldsymbol{H}_{\text{TDOA}} = \begin{bmatrix} \left(\boldsymbol{s}_2^T - \boldsymbol{s}_1^T\right) & r_{21} \\ \left(\boldsymbol{s}_3^T - \boldsymbol{s}_1^T\right) & r_{31} \\ \vdots & \vdots \\ \left(\boldsymbol{s}_N^T - \boldsymbol{s}_1^T\right) & r_{N1} \end{bmatrix}, \quad \boldsymbol{a}_{\text{TDOA}} = \frac{1}{2}\begin{bmatrix} K_{21} - r_{21}^2 \\ K_{31} - r_{31}^2 \\ \vdots \\ K_{N1} - r_{N1}^2 \end{bmatrix}.$$

and $K_{i1} = \|\boldsymbol{s}_2\|^2 - \|\boldsymbol{s}_1\|^2$, $i = 2, \ldots, N$. Providing that $\boldsymbol{H}_{\text{TDOA}}$ is a full column rank matrix, the LS estimator of $\boldsymbol{\theta}_{\text{TDOA}}$ is given by

$$\hat{\boldsymbol{\theta}}_{\text{TDOA}}^{\text{LS}} = \left(\boldsymbol{H}_{\text{TDOA}}^T\boldsymbol{H}_{\text{TDOA}}\right)^{-1}\boldsymbol{H}_{\text{TDOA}}^T\boldsymbol{a}_{\text{TDOA}}. \tag{9}$$

Now, observing that the three components of the vector $\boldsymbol{\theta}$ in (8) are functionally dependent to each other, i.e. $r_1 = \|\boldsymbol{u}\|$, it is

of interest to reconsider (8) enforcing the following constraint set

$$\begin{cases} \boldsymbol{\theta}_{\text{TDOA}}^T \boldsymbol{C} \boldsymbol{\theta}_{\text{TDOA}} = 0 \\ r_1 \geq 0 \end{cases}, \tag{10}$$

where

$$\boldsymbol{C} = \begin{bmatrix} 1 & 0 & 0 \\ 0 & 1 & 0 \\ 0 & 0 & -1 \end{bmatrix}. \tag{11}$$

A solution to the above constraint optimization problem can be found according to the CLS estimation procedure provided in [4], namely

$$\widehat{\boldsymbol{\theta}}_{\text{CLS}}(\eta^\star) = \left(\boldsymbol{H}_{\text{TDOA}}^T \boldsymbol{H}_{\text{TDOA}} + \eta^\star \boldsymbol{C} \right)^{-1} \boldsymbol{H}_{\text{TDOA}}^T \boldsymbol{a}_{\text{TDOA}}, \tag{12}$$

where $\eta^\star \in \mathbb{R}$ is chosen among the roots of $\widehat{\boldsymbol{\theta}}_{\text{CLS}}^T(\eta^\star) \boldsymbol{C} \widehat{\boldsymbol{\theta}}_{\text{CLS}}(\eta^\star) = 0$, based on the solution of a fourth order polynomial equation [4].

III. TOA/TDOA Applied to AIS

As discussed in Section II, both TOA and TDOA localization methods require precise time synchronization among the nodes of the passive localization system. Furthermore, TOA-based localization algorithms also require accurate knowledge of τ_0, i.e., the time instant when the signal is transmitted by the source to be localized.

In the context of passive localization of AIS sources, the previous requirements can be effectively met by leveraging the channel access scheme inherent to AIS. Specifically, AIS operates using a Time Division Multiple Access (TDMA) scheme, in which time is divided into frames and slots that are synchronized with the Coordinated Universal Time (UTC). A frame lasts 60 s, aligns with the start of a UTC minute, and is further divided into 2250 time slots, with AIS transmissions scheduled to occur in one or more consecutive slots (see Figure 1). This structured transmission scheme requires accurate time synchronization among all AIS-equipped units, typically achieved through Global Navigation Satellite System (GNSS) receivers that provide high-precision timing references.

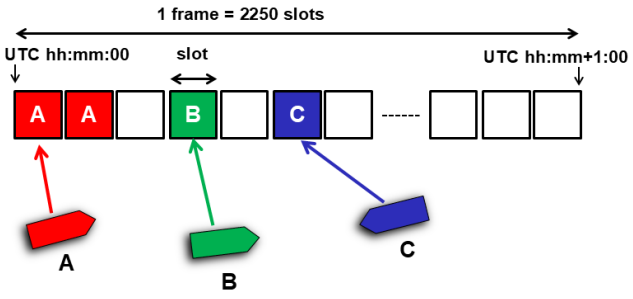


Fig. 1. AIS channel TDMA scheme: each frame is divided into 2250 slots of 26.67 ms, used for AIS message transmissions.

The time synchronization inherent in the AIS infrastructure enables the use of multiple shore-based AIS BSs as nodes in a TOA- and TDOA-based passive localization system, thereby eliminating the need for additional hardware. These AIS BSs are already deployed within the existing AIS network and are primarily used to receive and decode transmissions for vessel tracking and maritime traffic monitoring. As previously discussed, they are synchronized to a common time reference, which satisfies the time synchronization requirement essential for both TOA and TDOA techniques. By equipping the BSs with the capability to measure the TOA of AIS signals transmitted by vessels, they can also operate as passive receivers for localization purposes without requiring substantial modifications to the current infrastructure.

Regarding the transmission time τ_0 required by TOA-based localization techniques, and according to the AIS specification, it is reasonable to assume that AIS signals from vessels are transmitted at the beginning of their assigned time slots. This assumption enables the practical application of TOA-based localization methods without requiring explicit knowledge of τ_0, which can be inferred as

$$\tau_0 = t_s + (N_s - 1) T_s, \tag{13}$$

where $T_s \approx 27$ ms is the duration of a slot, while t_s and $N_s \in \{1, \ldots, 2250\}$ denote the UTC time marking the beginning of the frame and the slot number in which the AIS signal is transmitted, respectively.

Before concluding this section, it is worth pointing out that the Italian AIS BSs are equipped with TOA measurement capabilities featuring a temporal granularity of 1 μs. The measured TOA is computed not at the exact beginning of the AIS time slot, but after a delay corresponding to 40 bits from its start. These 40 bits comprise the preamble used for time synchronization with the AIS data field. As a result, at the ith BS used for passive localization, the actual TOA of an AIS signal can be inferred as

$$\tau_i = \tilde{\tau}_i - 40 T_b, \quad i = 1, \ldots, N, \tag{14}$$

where $\tilde{\tau}_i$ is the TOA measured at the ith BS, and $T_b \approx 104$ μs denotes the bit duration.

Based on the above discussion, Figure 2 summarizes the TOA/TDOA-based passive localization of AIS-equipped vessels using multiple shore-based AIS BSs.

IV. Performance Analysis

The performance is assessed in a real-world scenario by considering an AIS-based passive localization system composed of four BSs. Specifically, the BSs are located in southern Italy at Monte Redentore (40.6561° N, 17.2889° E), Monte San Michele (39.2861° N, 16.9794° E), Salento Turrisi (40.0621° N, 18.1424° E), and Stigliano (40.3955° N, 16.2321° E). The deployment of these BSs is illustrated in Figure 3, where $\mathbf{s}_i$, $i = 1, \ldots, 4$, includes the coordinates of each BS.

The analysis is aimed at studying: 1) the localization performance of the LS-TOA, LS-TDOA, and CLS-TDOA methods;

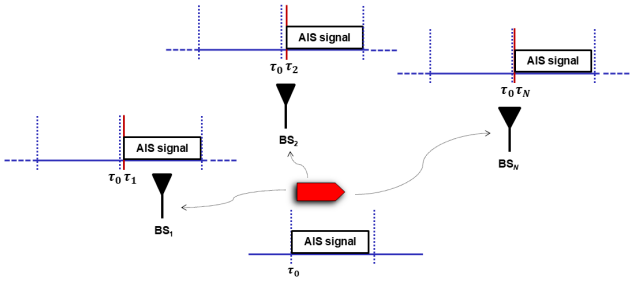


Fig. 2. Pictorial representation of the TOA/TDOA-based passive localization of AIS-equipped vessels using multiple shore-based AIS BSs.

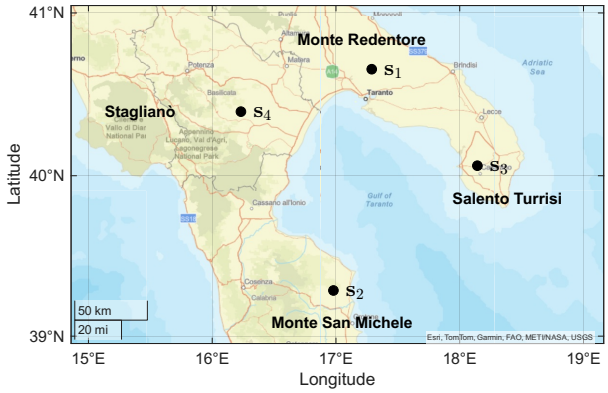


Fig. 3. Geometric configuration of the four used for passive localization.

and 2) the impact of the sensor geometry on the achievable localization accuracy. For both assessments, performance is quantified by the Root Mean Square Error (RMSE), defined as

$$\text{RMSE} = \sqrt{\frac{1}{M}\sum_{m=1}^{M} \|\hat{\boldsymbol{u}}_m - \boldsymbol{u}_m\|^2},$$

where $\boldsymbol{u}_m$ and $\hat{\boldsymbol{u}}_m$, $m = 1, \ldots, M$, denote the true and estimated vessel positions, respectively. For the purposes of the following assessment, the true positions are extracted from the processed AIS data messages.

A. TOA vs TDOA vs CLS-TDOA

The result of the comparison between the LS-based TOA, TDOA, and CLS-TDOA techniques is illustrated in Figure 4, which displays the estimated vessel positions overlaid on a topographic map of the area of interest. In each subplot, black dots denote the positions of the receiving stations, blue dots indicate the true vessel positions, and red dots represent the position estimates produced by each algorithm.

Visual inspection of the topographic maps reveals that the CLS-TDOA algorithm yields position estimates that are almost always closer to the true vessel locations than those produced by the LS-TOA and LS-TDOA methods. As anticipated, the LS-TOA algorithm demonstrates the lowest performance, primarily due to its reliance on absolute time-of-arrival measurements, which makes it highly sensitive to clock synchronization errors and measurement noise.

To further analyze the localization accuracy, Figure 5 reports the histograms of the absolute position estimation errors along the two coordinate axes. The top, middle, and bottom rows correspond to the LS-TOA, LS-TDOA, and CLS-TDOA algorithms, respectively, while the left and right columns show the error distributions along the x-axis and y-axis, respectively. The histograms of the estimation errors reveal important details about the statistical behavior of the algorithms. In fact, the LS-TOA shows broader error distributions in both x and y, suggesting less precision. The LS-TDOA instead generally improves upon the LS-TOA by removing the need for absolute time synchronization between stations, but still exhibits larger tails in the histograms, indicating occasional larger errors. Differently, the CLS-TDOA produces narrower histograms, with most of the error mass concentrated near zero, reflecting both higher accuracy and greater stability than its counterparts. These trends are quantitatively confirmed by the RMSE values reported in Table I, where the overall Two-Dimensional (2D) positional RMSE, as well as the RMSE of the position components along the x and y axes are summarized. As expected, the CLS-TDOA algorithm, which incorporates prior constraints, achieves the best performance in terms of estimation accuracy, especially in challenging geometric configurations with a limited number of receiving stations.

TABLE I
RMSE VALUES OF POSITION ESTIMATES

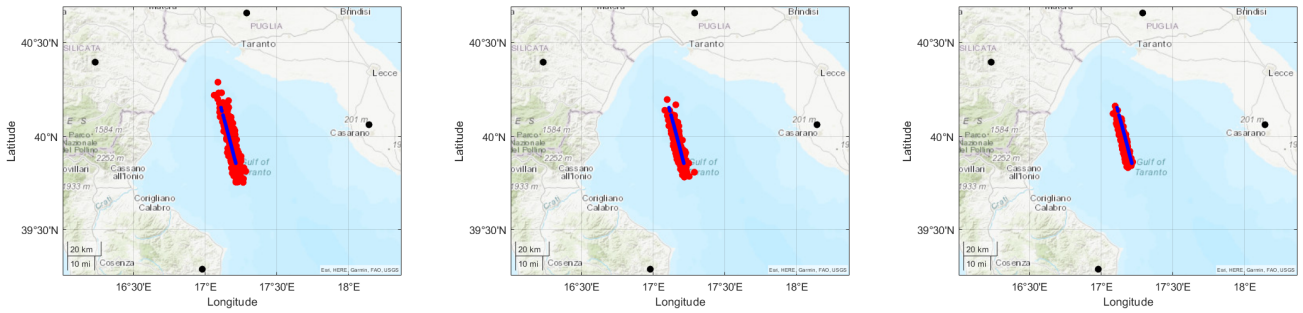
Algorithm	**RMSE**(x_u) **[km]**	**RMSE**(y_u) **[km]**	**RMSE [km]**
LS-TOA	5.56	2.05	5.93
LS-TDOA	2.46	1.48	2.88
CLS-TDOA	1.60	1.51	2.20

B. Impact of Sensor Geometry

The objective of this analysis is to investigate the dependence of the achievable localization performance on the geometric configuration of the sensors. Since the available network is composed of four sensors, different deployments can be studied by considering all possible triplets of three sensors, which are: $(\boldsymbol{s}_1, \boldsymbol{s}_2, \boldsymbol{s}_3)$ (case 1), $(\boldsymbol{s}_1, \boldsymbol{s}_2, \boldsymbol{s}_4)$ (case 2), $(\boldsymbol{s}_1, \boldsymbol{s}_3, \boldsymbol{s}_4)$ (case 3), and $(\boldsymbol{s}_2, \boldsymbol{s}_3, \boldsymbol{s}_4)$ (case 4). This allows evaluating how the choice of sensor placement affects the estimation accuracy. The study focuses on TOA-based localization techniques, while the evaluation of TDOA methods is left for future work.

For the purpose of this assessment, the scenario in Figure 6 is considered, where the position of the vessel to be localized can be assumed to remain almost fixed with respect to the acquisition geometry. This assumption allows the analysis to focus exclusively on the impact of sensor placement, without introducing additional variability due to the target motion.

From a theoretical point-of-view, the impact of sensor deployment on the achievable performance can be studied



(a) LS-TOA (b) LS-TDOA (c) CLS-TDOA

Fig. 4. Results of the LS-TOA, LS-TDOA, and CLS-TDOA positioning algorithms visualized on the topographic map.

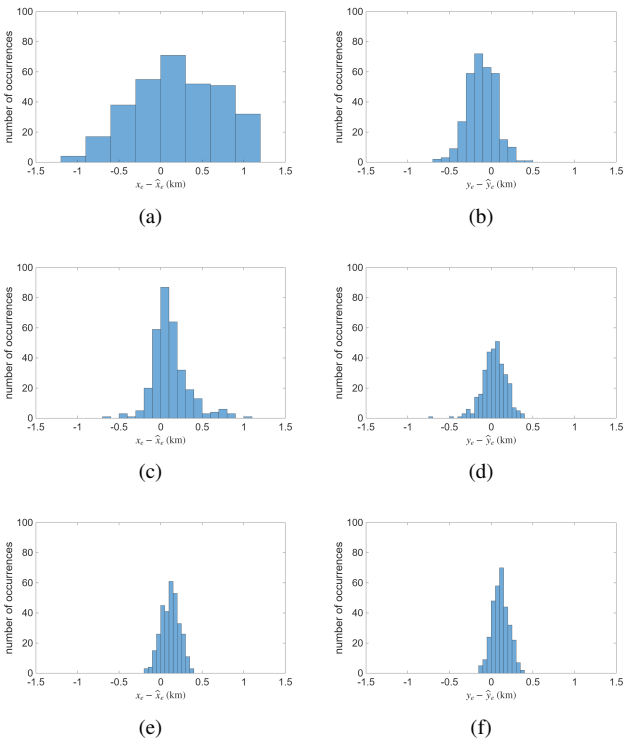


Fig. 5. Histograms of the absolute position estimation errors for the LS-TOA (top line), LS-TDOA (central line), and CLS-TDOA (bottom line) algorithms along the x- (left) and y-axes (right).

via the Cramér–Rao Bound (CRB). For TOA-based passive localization, the CRB matrix, which provides a lower bound to the covariance matrix of any unbiased estimator of the target position, is given by [9]

$$\boldsymbol{C}_{\mathrm{TOA}}(\boldsymbol{u}, \boldsymbol{s}_1, \ldots, \boldsymbol{s}_N) = \left(\boldsymbol{A}^T \boldsymbol{R}_{\mathrm{TOA}}^{-1} \boldsymbol{A}\right)^{-1}, \qquad (15)$$

where the dependence on the actual target position $\boldsymbol{u}$ and the sensor locations $\boldsymbol{s}_1, \ldots, \boldsymbol{s}_N$ is introduced through the matrix $\boldsymbol{A}$, defined as

$$\boldsymbol{A} = \left[\frac{\boldsymbol{u} - \boldsymbol{s}_1}{\|\boldsymbol{u} - \boldsymbol{s}_1\|}, \ \ldots, \ \frac{\boldsymbol{u} - \boldsymbol{s}_N}{\|\boldsymbol{u} - \boldsymbol{s}_N\|}\right]^T. \qquad (16)$$

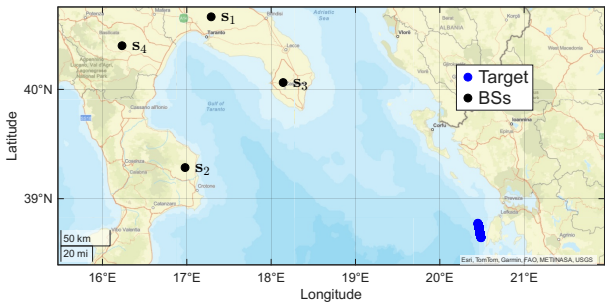


Fig. 6. Map of the scenario used for evaluating the impact of the sensor geometry.

In (15), the matrix $\boldsymbol{R}_{\mathrm{TOA}} = \mathrm{diag}\left(\sigma_1^2, \sigma_2^2, \ldots, \sigma_N^2\right)$ denotes the measurement noise covariance matrix, with σ_n^2, $n = 1, \ldots, N$, representing the variance of the TOA measurement error at the n-th sensor.

Hence, Figure 7 shows the trace of the CRB matrix corresponding to each target position and sensor deployment. In this assessment, thanks to the availability of the true position of the vessel, as provided by the received AIS messages, the values of σ_n^2, $n = 1, \ldots, N$, involved in the CRB matrix have been estimated from the available TOA measurements.

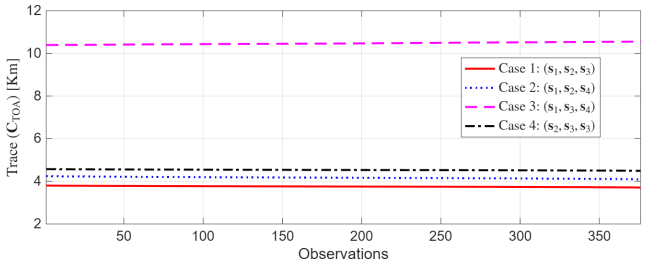


Fig. 7. Trace of the CRB for varying target positions under different sensor configurations.

Since the position of the vessel can be assumed to be stationary with respect to the available sensor geometries, the obtained curves confirm that, for a given sensor configuration, the theoretical performance is almost constant with respect to the target location. Additionally, the curves also indicate

that case 1 provides the best theoretical performance, followed respectively by case 2, case 4, and case 3.

It is now worth observing that, the intrinsic structure of the LS solution may introduce estimation bias due to algebraic approximation. Thus, the impact of the configuration on the performance is also evaluated using the (asymptotically unbiased) Gauss–Newton (GN) algorithm [14], which directly addresses the nonlinear LS problem by iteratively refining the position estimate through local linearizations of the measurement model.

Table II compares the obtained RMSEs with the average trace of the CRB matrix. For the LS-based approach, the results partially confirm the theoretical trend. Indeed, while for cases 1 and 3 the RMSE is consistent with the CRB ranking, for cases 2 and 4 an inverted trend is observed. As mentioned before, this discrepancy is likely due to the estimation bias of the LS approach. On the other hand, the RMSEs obtained via the GN algorithm closely align with the CRB for all sensor triplets, confirming that the mismatch observed with the LS method originates from its approximate formulation.

Overall, these results emphasize the critical role of sensor placement in TOA localization. Specifically, different sensor network geometries can lead to variations in localization performance. This motivates the development of bespoke methods that enable the optimal placement of sensors to enhance localization accuracy [9].

TABLE II
RMSE VALUES COMPARED TO THE CRB FOR DIFFERENT CONFIGURATIONS OF THE SENSORS

Case	RMSE LS [km]	RMSE GN [km]	CRB [km]
1	10.26	10.97	3.76
2	21.96	11.67	4.17
3	22.78	19.76	10.47
4	15.11	11.39	4.53

V. CONCLUSIONS

This paper has investigated the use of TOA- and TDOA-based localization methods for maritime surveillance by leveraging timestamp information provided by the Italian AIS network. In addition, it has addressed the impact of the geometry of the localization network on the achievable performance. The former study has been carried out considering three passive localization techniques, namely LS-TOA, LS-TDOA, and CLS-TDOA. The latter, instead, has focused exclusively on TOA-based localization methods.

The experimental results have shown that TDOA-based localization techniques outperform TOA-based method, as they inherently are not sensible to synchronization errors due to the unknown transmission time. Among the TDOA approaches, the CLS-TDOA algorithm further improves localization accuracy as compared with the classical LS-based method, thanks to the inclusion in the optimization process of a suitable constraint that accounts for the relationship between the estimation variables. These findings have highlighted the importance of incorporating bespoke constraints into localization frameworks to enhance estimation accuracy under realistic operating conditions. Moreover, the analysis has highlighted a strong dependence of localization performance on sensor geometry, in agreement with the trends predicted by the CRLB. These findings not only validate the theoretical predictions but also emphasize the importance of carefully designing the sensor deployment to achieve optimal performance in passive localization systems.

Future research might focus on extending the conducted assessment to additional case studies and larger sensor networks, as well as evaluating the impact of sensor geometry on TDOA-based localization techniques.

ACKNOWLEDGMENTS

The authors are grateful to the Italian Coast Guard Headquarters for providing the AIS data used along this study.

REFERENCES

[1] B. Friedlander, "A Passive Localization Algorithm and its Accuracy Analysis," *IEEE Journal of Oceanic Engineering*, vol. 12, no. 1, pp. 234–245, January 1987.

[2] Y. T. Chan and K. C. Ho, "A Simple and Efficient Estimator for Hyperbolic Location," *IEEE Transactions on Signal Processing*, vol. 42, no. 8, pp. 1905–1915, August 1994.

[3] K. C. Ho and W. Xu, "An Accurate Algebraic Solution for Moving Source Location using TDOA and FDOA Measurements," *IEEE Transactions on Signal Processing*, vol. 52, no. 9, pp. 2453–2463, September 2004.

[4] A. Beck, P. Stoica, and J. Li, "Exact and Approximate Solutions of Source Localization Problems," *IEEE Transactions on Signal Processing*, vol. 56, no. 5, pp. 1770–1778, May 2008.

[5] J. Shen, A. Molisch, and J. Salmi, "Accurate Passive Location Estimation Using TOA Measurements," *IEEE Transactions on Wireless Communications*, vol. 11, no. 6, pp. 2182–2192, June 2012.

[6] A. Aubry, V. Carotenuto, A. De Maio, and L. Pallotta, "Joint Exploitation of TDOA and PCL Techniques for Two-Dimensional Target Localization," *IEEE Transactions on Aerospace and Electronic Systems*, vol. 56, no. 1, pp. 597–609, 2020.

[7] ——, "Localization in 2D PBR With Multiple Transmitters of Opportunity: A Constrained Least Squares Approach," *IEEE Transactions on Signal Processing*, vol. 68, pp. 634–646, 2020.

[8] L. Pallotta and G. Giunta, "Accurate Delay Estimation for Multisensor Passive Locating Systems Exploiting the Cross-Correlation Between Signals Cross-Correlations," *IEEE Transactions on Aerospace and Electronic Systems*, vol. 58, no. 3, pp. 2568–2576, 2022.

[9] A. Aubry, P. Babu, A. De Maio, G. Fatima, and N. Sahu, "A Robust Framework to Design Optimal Sensor Locations for TOA or RSS Source Localization Techniques," *IEEE Transactions on Signal Processing*, vol. 71, pp. 1293–1306, 2023.

[10] F. Papi, D. Tarchi, M. Vespe, F. Oliveri, F. Borghese, G. Aulicino, and A. Vollero, "Radiolocation and Tracking of Automatic Identification System Signals for Maritime Situational Awareness," *IET Radar, Sonar & Navigation*, vol. 9, no. 5, pp. 568–580, 2015.

[11] S. Ma, J. Wang, X. Meng, and J. Wang, "A Vessel Positioning Algorithm Based on Satellite Automatic Identification System," *Journal of Electrical and Computer Engineering*, vol. 2017, no. 1, p. 8097187, 2017.

[12] C. Gioia, F. Sermi, and D. Tarchi, "Multi-Network Asynchronous TDOA Algorithm Test in a Simulated Maritime Scenario," *Sensors*, vol. 20, no. 7, 2020. [Online]. Available: https://www.mdpi.com/1424-8220/20/7/1842

[13] M. Delcourt and J.-Y. Le Boudec, "TDOA Source-Localization Technique Robust to Time-Synchronization Attacks," *IEEE Transactions on Information Forensics and Security*, vol. 16, pp. 4249–4264, 2021.

[14] L. A. Romero and J. Mason, "Evaluation of Direct and Iterative Methods for Overdetermined Systems of TOA Geolocation Equations," *IEEE Transactions on Aerospace and Electronic Systems*, vol. 47, no. 2, pp. 1213–1229, 2011.